GRAVITATIONAL LENSING

9- GRAVITATIONAL MICROLENSING II : STATISTICS

R. Benton Metcalf

2022-2023

MICROLENSING LIGHT CURVE

magnification

$$\mu(y) = \frac{y^2 + 2}{y\sqrt{y^2 + 4}}$$

$$y(t) = \sqrt{y_o^2 + y_1(t)^2} = \sqrt{y_o^2 + \frac{(t - t_o)^2}{t_E^2}}$$

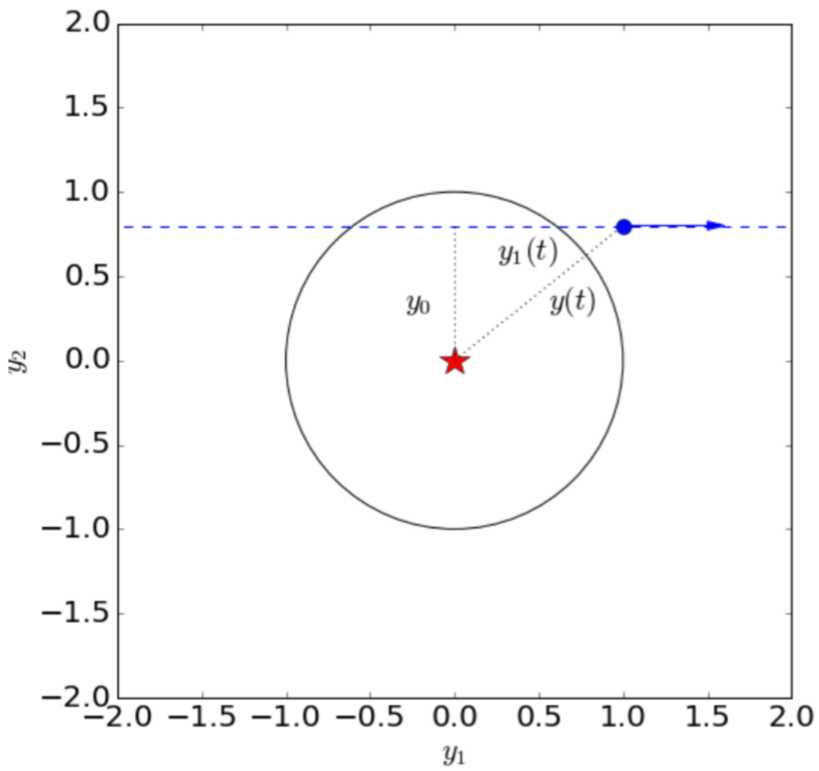

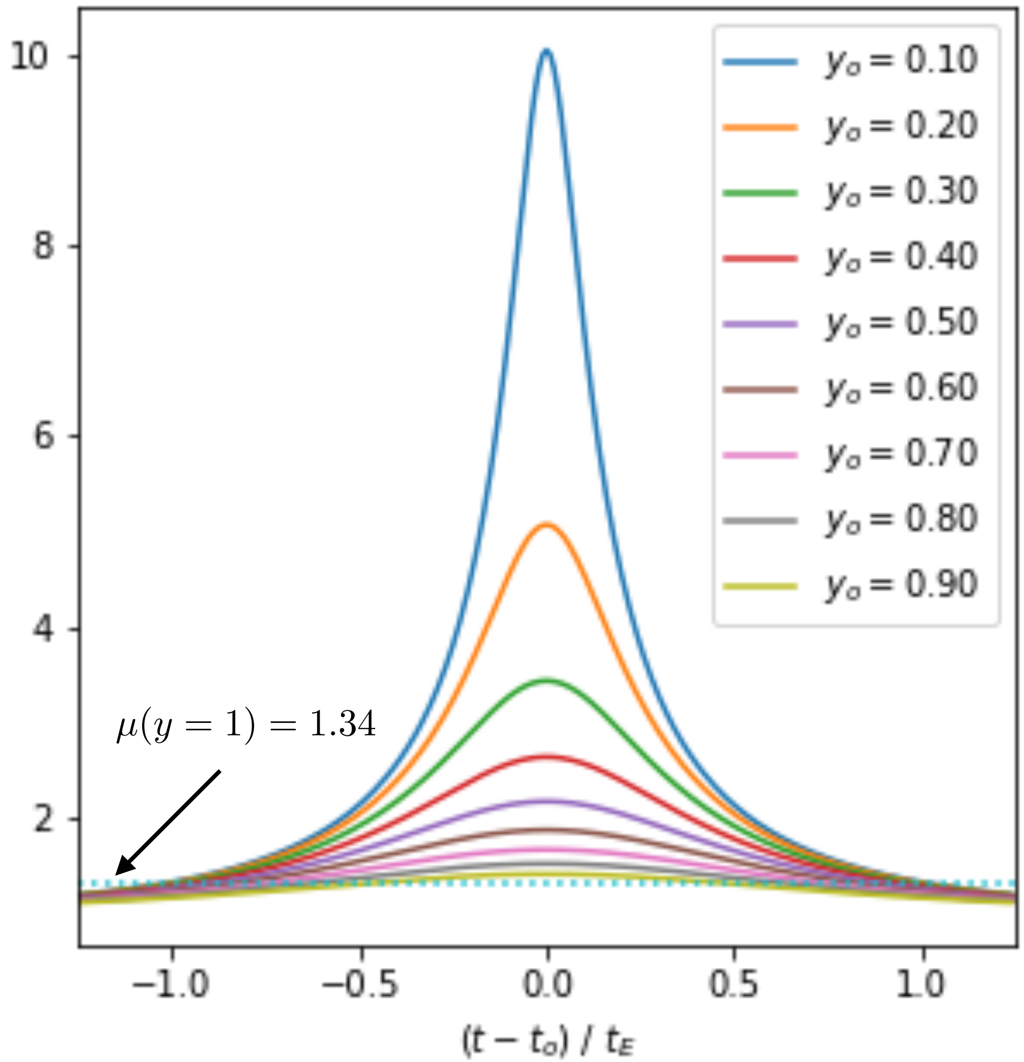

MICROLENSING STATISTICS

Einstein radius

$$R_E = D_l \theta_E = \sqrt{\frac{4GM}{c^2} \frac{D_{ls} D_l}{D_s}} = \sqrt{\frac{4GM}{c^2} D_s x (1-x)}$$

Einstein crossing time

$$t_E = \frac{R_E}{|v_\perp|}$$

OPTICAL DEPTH - probability that a star is being microlensed.

$$\tau = \frac{4\pi G}{c^2} D_s^2 \int_0^1 dx \; x(1-x)\, \rho(x D_s)$$

EVENT RATE

$$\Gamma = 2N_* \int_0^{D_s} dD \int_0^\infty dM \int d^3v \; f(v) f(M) \; |v_\perp| R_E(M,D) \frac{\rho(D)}{M}$$

$$= 2N_* \sqrt{\frac{4G}{c^2}} D_s^{3/2} \int_0^\infty dM \int_0^1 dx f(M) \; \sqrt{\frac{x(1-x)}{M}} \rho(D_s x) \; \langle |v_\perp| \rangle$$

MICROLENSING STATISTICS

Einstein radius

$$R_E = D_l \theta_E = \sqrt{\frac{4GM}{c^2}\frac{D_{ls}D_l}{D_s}} = \sqrt{\frac{4GM}{c^2}D_s x(1-x)}$$

Einstein crossing time

$$t_E = \frac{R_E}{|v_\perp|}$$

Einstein crossing time distribution

$$\frac{d\Gamma}{dt_E} = -2N_* \int_0^{D_s} dD \int_0^\infty dM f(M) f_v\left(\frac{R_E}{t_E}\right) \left(\frac{R_E}{t_E}\right)^3 \frac{\rho(D)}{M}$$

For an isotropic Maxwellian velocity distribution $f_v(v_\perp) = \frac{v_\perp}{\sigma^2}\exp\left[-\frac{v_\perp^2}{2\sigma}\right]$

$$\frac{d\Gamma}{dt_E} = -\frac{2N_*}{\sigma^2}\frac{1}{t_E^4}\int_0^{D_s} dD \int_0^\infty dM f(M)\ R_E^4\ \frac{\rho(D)}{M}\ \exp\left[-\frac{1}{2\sigma^2}\left(\frac{R_e}{t_E}\right)^2\right]$$

MICROLENSING STATISTICS

$D_s = 8 \text{ kpc}$

$\sigma_v = 120 \text{ km/s}$ *Gaussian distributed*

$\rho(D) = \text{const.}$

$f(M') = \delta_D(M' - M)$ *mass distribution*

$$t_E^{\max} \sim \frac{t_o}{5.25} = 0.38\sqrt{\frac{GMD_s}{c^2\sigma^2}}$$

$$\frac{1}{\Gamma}\frac{d\Gamma}{d\ln t_E}$$

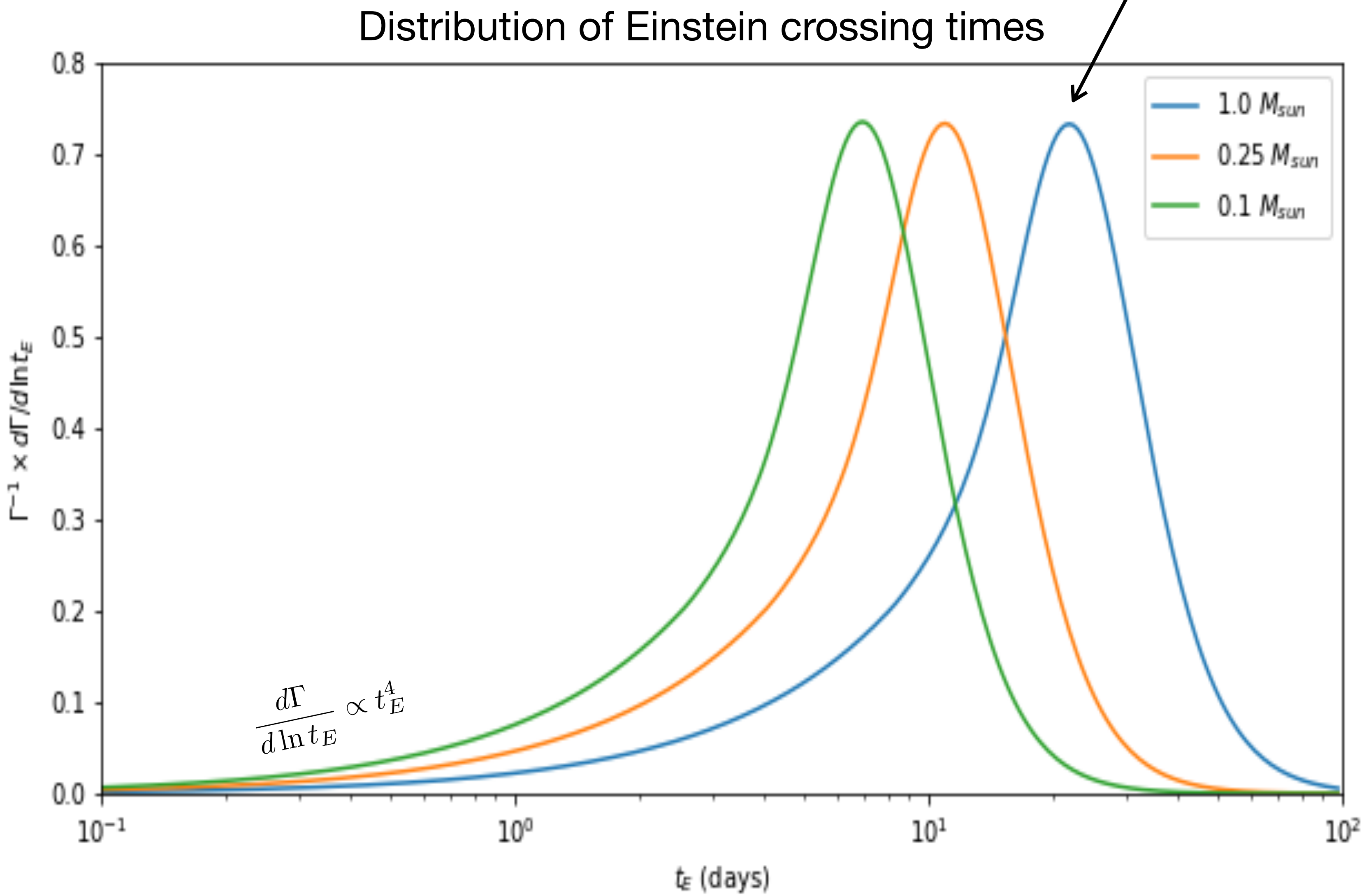

A MODEL FOR OUR GALAXY

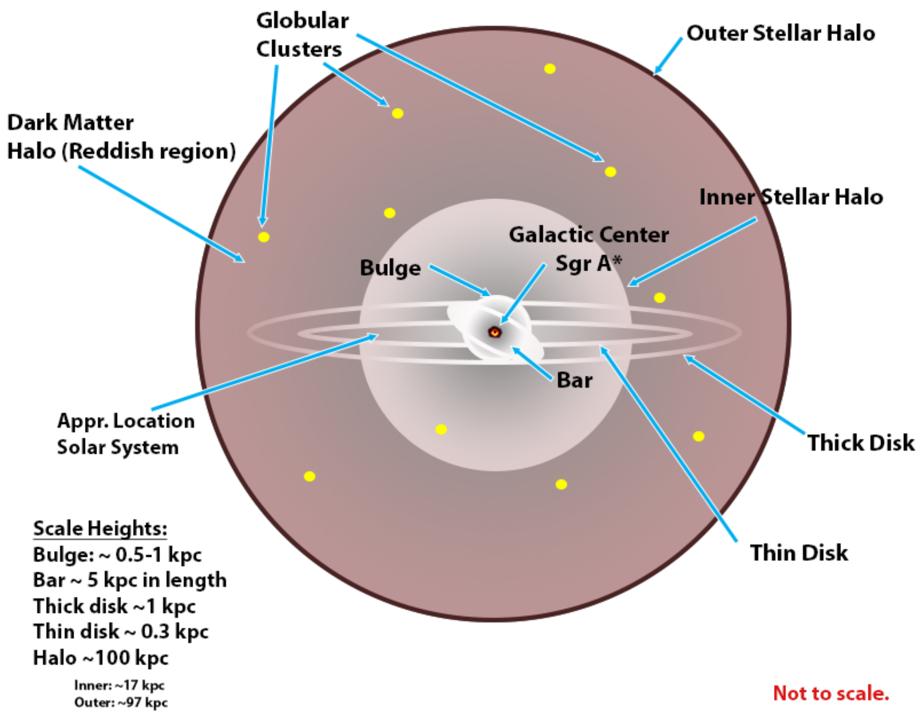

All these components have their own optical depths...

I) thin & thick disk (young stars & gas)

$$\rho^D(R,z) = \rho_0^D \exp\left(-\frac{R-R_0}{h_R} - \frac{|z|}{h_z}\right)$$

$$\sigma^D \simeq 20 \text{ km/s} \qquad v_{rot}^D \simeq 220 \text{ km/s}$$

$$\sigma^{TD} \simeq 40 \text{ km/s} \qquad v_{rot}^{TD} \simeq 180 \text{ km/s}$$

II) Spheroid (old star halo)

$$\rho^S \propto r^{-3.5} \qquad \sigma^S \simeq 120 \text{ km/s}$$

III) Bulge (contains a bar)

$$\rho^B(s) = \frac{M_0}{8\pi abc} \exp\left[-\frac{s^2}{2}\right]$$

$$s^4 \equiv [(x'/a)^2 + (y'/b)^2]^2 + (z'/c)^4$$

A MODEL FOR OUR GALAXY

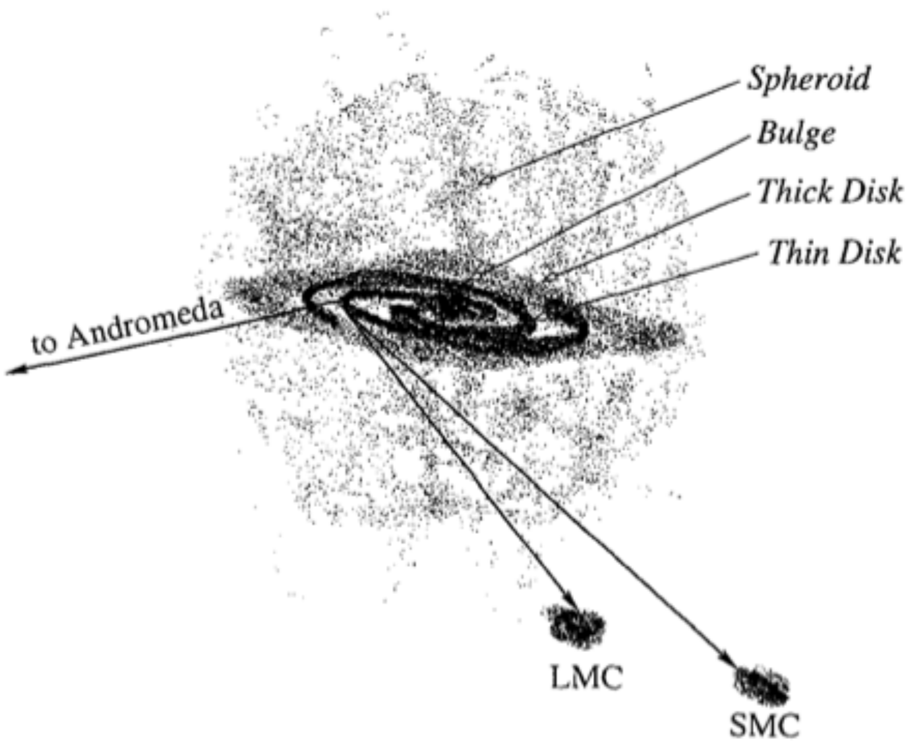

All these components have their own optical depths...

I) thin & thick disk (young stars & gas)

$$\rho^D(R,z) = \rho_0^D \exp\left(-\frac{R-R_0}{h_R} - \frac{|z|}{h_z}\right)$$

$$\sigma^D \simeq 20 \text{ km/s} \qquad v_{rot}^D \simeq 220 \text{ km/s}$$

$$\sigma^{TD} \simeq 40 \text{ km/s} \qquad v_{rot}^{TD} \simeq 180 \text{ km/s}$$

II) Spheroid (old star halo)

$$\rho^S \propto r^{-3.5} \qquad \sigma^S \simeq 120 \text{ km/s}$$

III) Bulge (contains a bar)

$$\rho^B(s) = \frac{M_0}{8\pi abc} \exp\left[-\frac{s^2}{2}\right]$$

$$s^4 \equiv [(x'/a)^2 + (y'/b)^2]^2 + (z'/c)^4$$

DIFFERENTIAL ROTATION

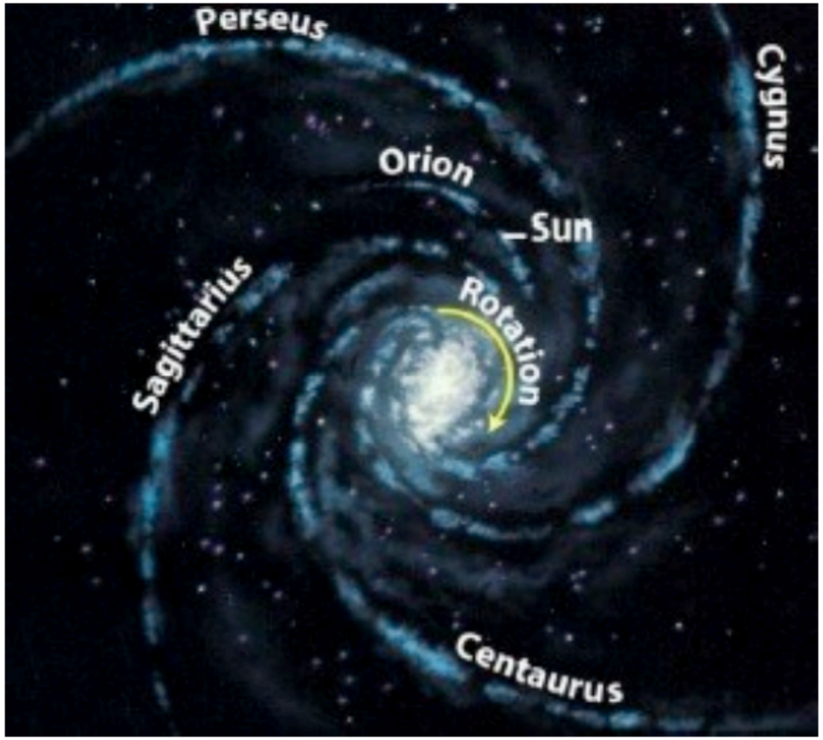

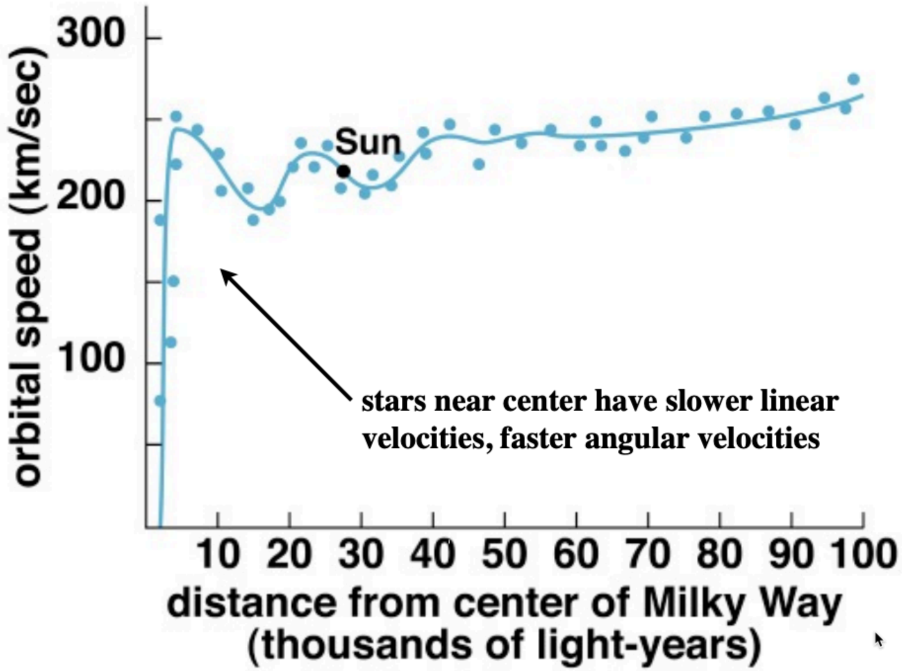

MICROLENSING SURVEYS: THE OGLE PROJECT

OGLE

The main OGLE Homepage

- Recent Scientific Results:
- Real Time Data Analysis Systems:
- OGLE Collection of Variable Stars [opens in new window]
- OGLE-II Photometry Databases [opens in new window]
- Main OGLE Results:
- Sky Coverage:
- GB Interstellar Extinction Calculator
- GB Microlensing Event Rate Maps
- Data Download Site
- Publications:
- OGLE related grants:
- Miscellaneus Information:
- Links to other Microlensing Teams: [opens in new window]
- OGLE Photo Gallery

- A free-floating or wide-orbit planet in the microlensing event OGLE-2019-BLG-0551
- Mapping the Northern Galactic Disk Warp with Classical Cepheids
- Over 78 000 RR Lyrae Stars in the Galactic Bulge and Disk
- Discovery of an Outbursting 12.8 Minute Ultracompact X-Ray Binary
- A three-dimensional map of the Milky Way using classical Cepheid variable stars
- OGLE Collection of Galactic Cepheids
- Microlensing optical depth and event rate toward the Galactic bulge from eight years of OGLE-IV observations
- 12 660 spotted stars toward the OGLE Galactic bulge fields
- Two new free-floating or wide-orbit planets from microlensing
- Rotation curve of the Milky Way from Classical Cepheids
- more...

OGLE-IV IN OPERATION

OGLE Variable Stars | On-line Data | Project description and history | Telescope information

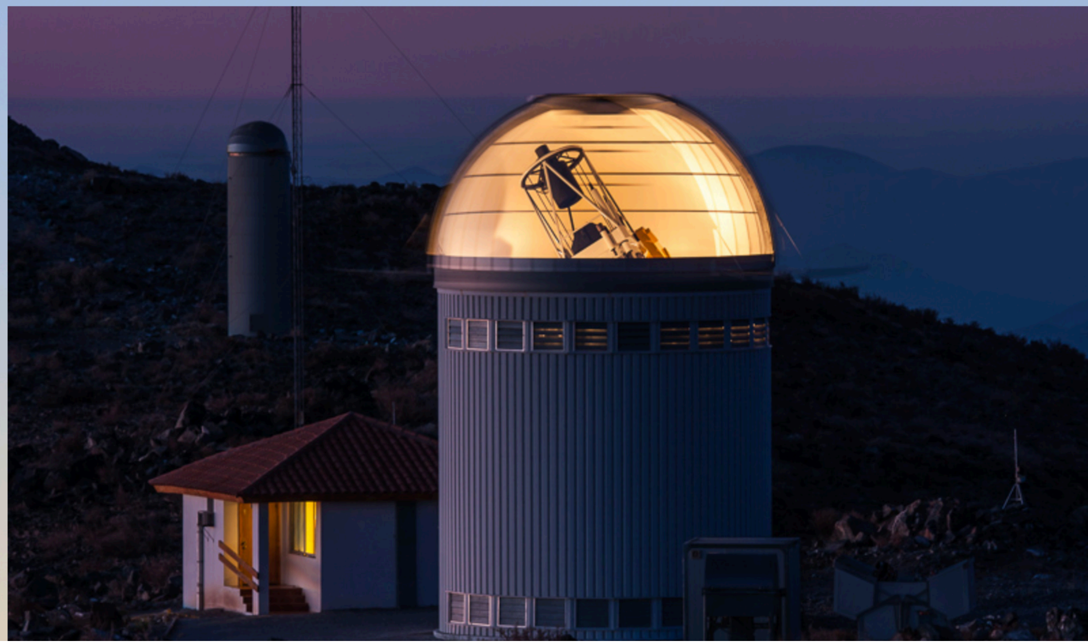

Main page   Coverage of the Sky   Coverage of the bulge

SKY COVERAGE

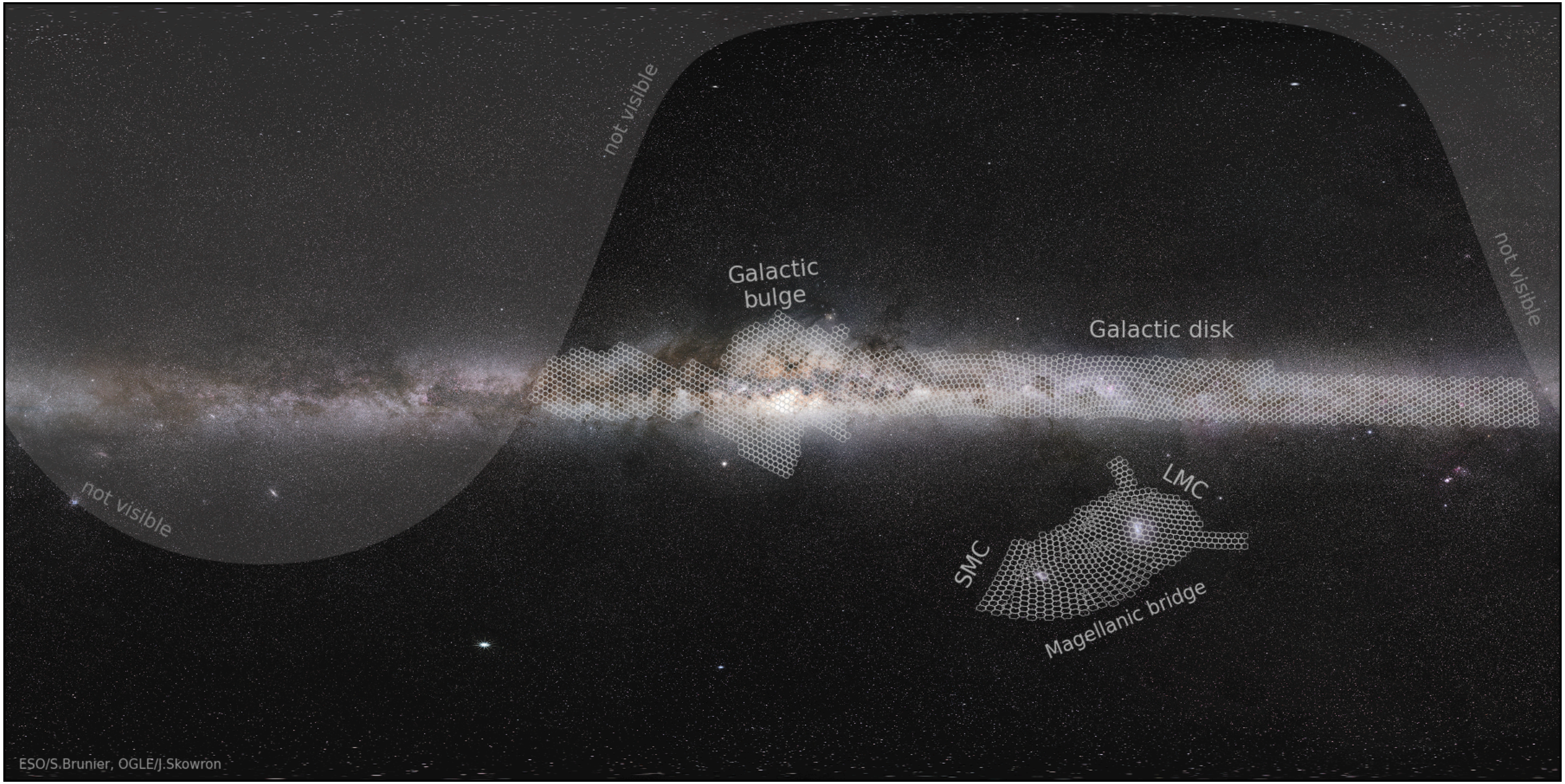

OPTICAL DEPTH AS A FUNCTION OF POSITION ON THE SKY

Unlike other probes of galactic structure, microlensing is sensitive to all stellar masses independently of distance.

The optical depth as a function of galactic coordinates gives a probe of different components of the galactic model.

The high rate and asymmetry towards the centre of the galaxy favour a galactic bar over a bulge.

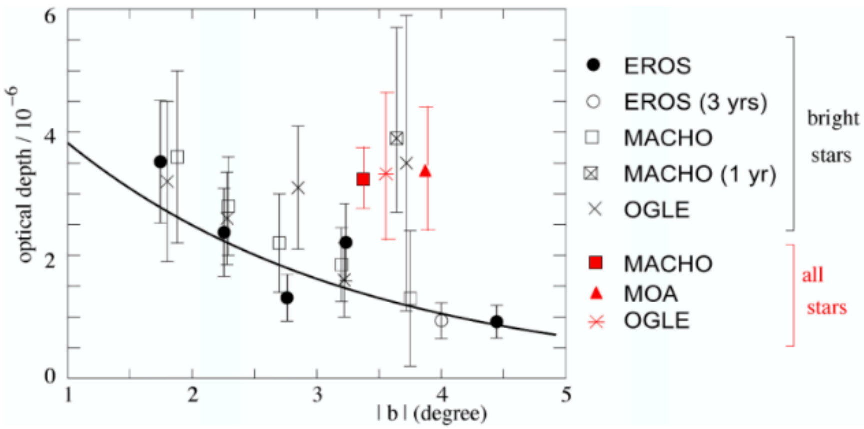

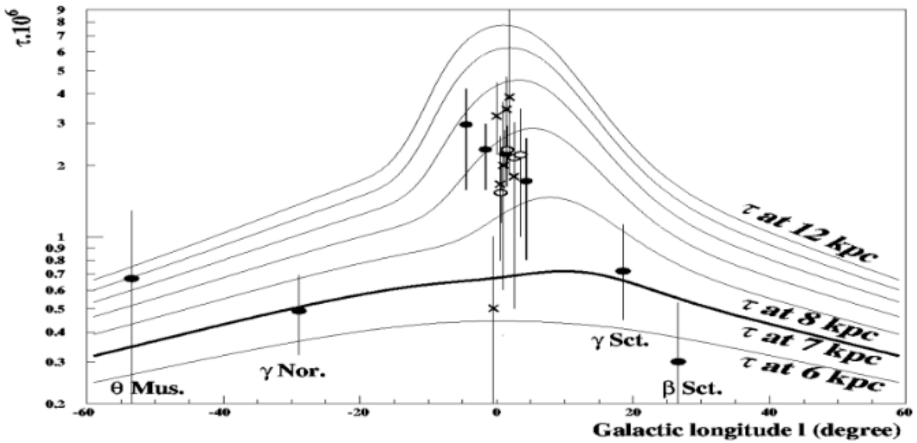

reference	sea-sons	field $deg.^2$	stars analyzed	events for τ	$\bar{l}^\circ, \bar{b}^\circ$	$<\tau>_{bulge}$ $\times 10^6$	$<t_E>$ corrected
OGLE [112]	2	0.81	all	9	$\pm 5, -3.5$	3.3 ± 1.2	
MACHO [11]	1	12.	all	45	$2.55, 3.64$	$3.9^{+1.8}_{-1.2}$	
MACHO [16]	3	4.	all/DIA	99	$2.68, -3.35$	$3.23^{+0.52}_{-0.50}$	
EROS [3]	3	15.	bright	16	$2.5, -4.0$	0.94 ± 0.29	
MOA [104]	1	18.	all/DIA	28	$4.2, -3.4$	$3.36^{+1.11}_{-0.81}$	
MACHO [86]	7	4.5	bright	62	$1.5, -2.68$	$2.17^{+0.47}_{-0.38}$	21.6 ± 3
OGLE [105]	4	5.	bright	32	$1.16, -2.75$	$2.55^{+0.57}_{-0.46}$	28.1 ± 4.3
EROS [62]	7	66.	bright	120	GC map		28.3 ± 2.8
EROS [87]	7	20.1	all	22	GSA map		$48. \pm 9.$

Moniez, 2010

LOW MASS INITIAL MASS FUNCTION

IMF IN THE BAR/BULGE SEEMS CONSTANT WITH THE LOCAL IMF.

$$dN = \Phi(\log M)\, d\log M \propto M^{-\alpha}\, dM \text{ where}$$
$$\alpha = \alpha_{\rm bd} \text{ for } 0.01\, M_\odot \leqslant M < 0.08\, M_\odot$$
$$\alpha = \alpha_{\rm ms} \text{ for } 0.08\, M_\odot \leqslant M < 0.5\, M_\odot = M_{\rm break}$$
$$\alpha = 2.3 \text{ for } 0.5\, M_\odot \leqslant M < 100\, M_\odot.$$

$\alpha_{\rm bd}$ brown dwarf slope

$\alpha_{\rm ms}$ main sequence slope

$$\Phi(\log M) \propto \exp\left\{\frac{-(\log M - \log M_c)^2}{2\sigma_m^2}\right\} \text{ for } M < 1.0 M_\odot$$
$$\alpha = 2.3 \text{ for } 1.0 M_\odot \leqslant M < 100 M_\odot.$$

OGLE-III *Wegg, Garhard & Portail, 2017 ApJL 843*

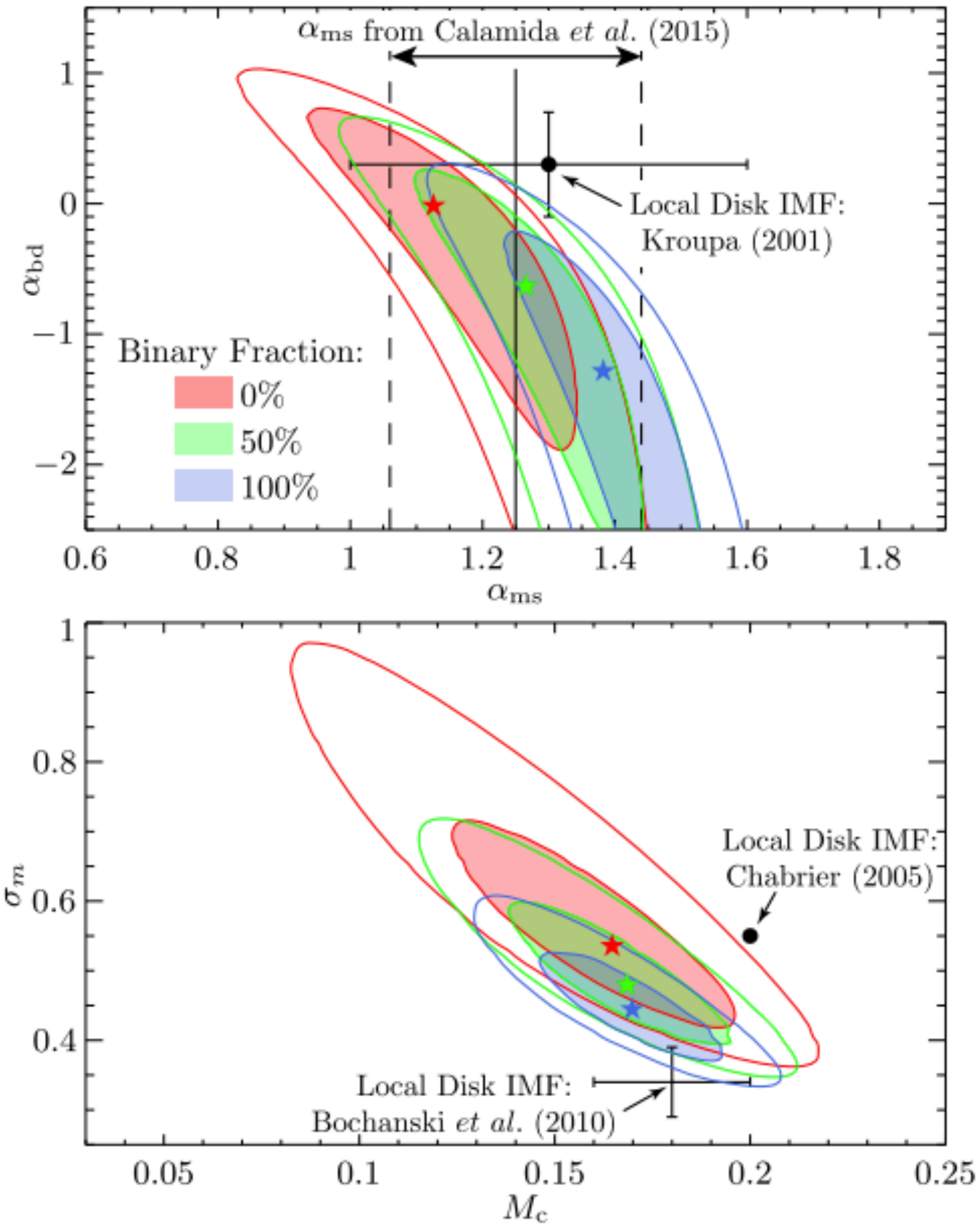

LIMITS ON MACHO DARK MATTER

Event rates toward the LMC and SMC rule out realistic halo models composed of Massive Compact Halo Objects (MACHOs) between the masses of 10^{-7} and 10 solar masses.

Only about 10% of a standard halo can consist of such objects.

Previously free floating "Jupiters" ($M < 0.01\ M_{sun}$ with time scales of a few hours to days) were the most plausible candidates for baryonic dark matter. They would be virtually undetectable otherwise.

Moniez, 2010

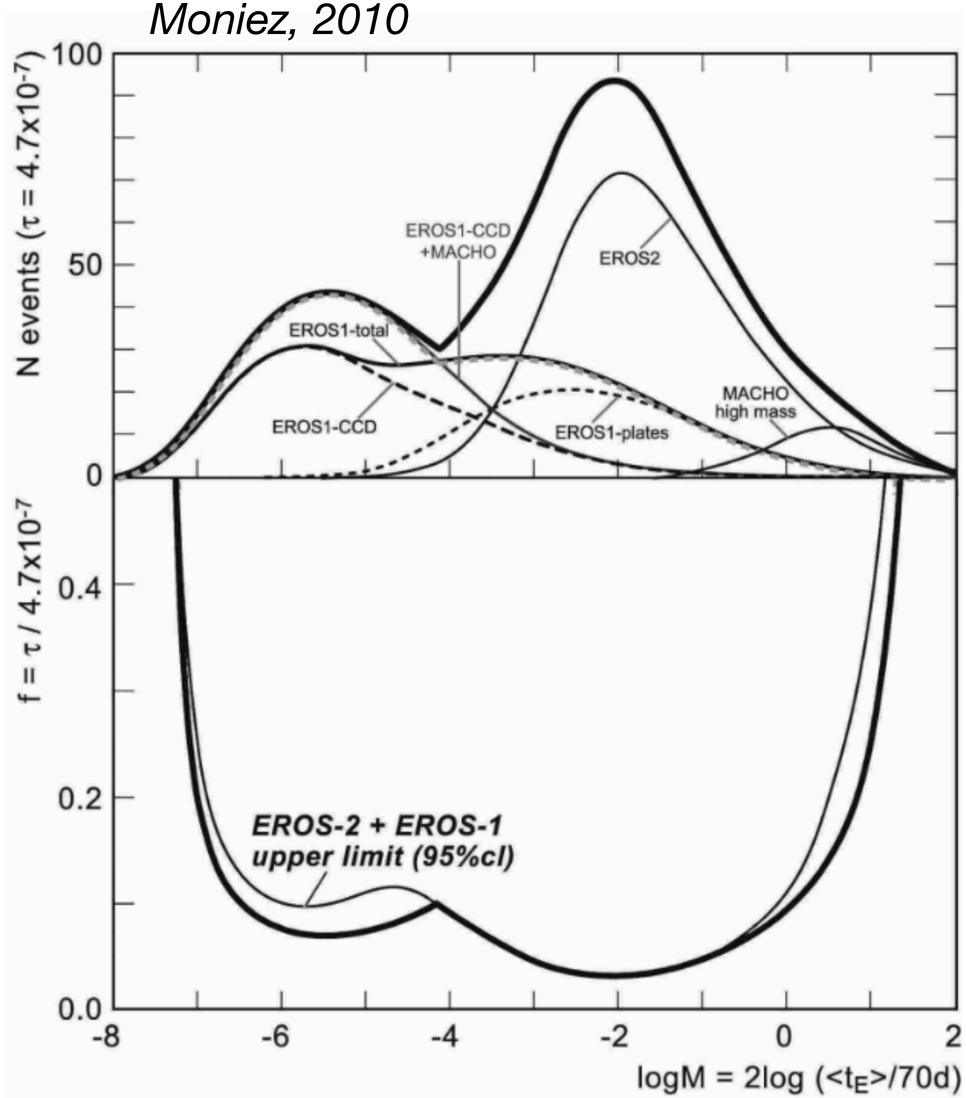

Fig. 7 *The top panel shows the number of expected events towards LMC as a function of the lens mass M for the S-model. The EROS1-total line shows the sum of the expectations from the CCD-camera and from the plates (dashed lines). The MACHO-high mass line corresponds to the "zero event" high mass search. The EROS1-CCD+MACHO line (blue) is the combined result from the EROS1 CCD-camera and the MACHO 2 year analysis. The grey dashed line is the envelope of the EROS1-total and the EROS1-CCD+MACHO lines. The final combination (thick line) is the sum of EROS2, of the grey dashed line and of half of the MACHO-high mass expectations (see text). In the lower panel, the thick line shows the combined 95% CL upper limit on $f = \tau_{LMC}/4.7 \times 10^{-7}$ based on no observed events. The thin line is the EROS1+EROS2 LMC limit.*

PROBING THE STELLAR POPULATIONS WITH MICROLENSING

Gaudi, 2012, Ann. Rev. Astron. Astrophys. 50, 411

Sumi et al 2011

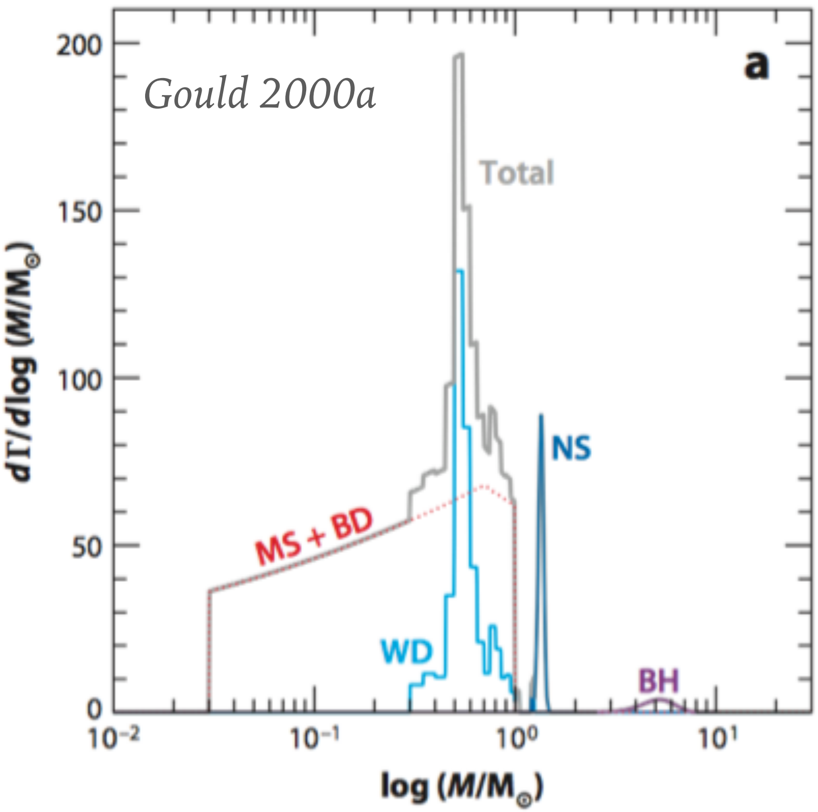

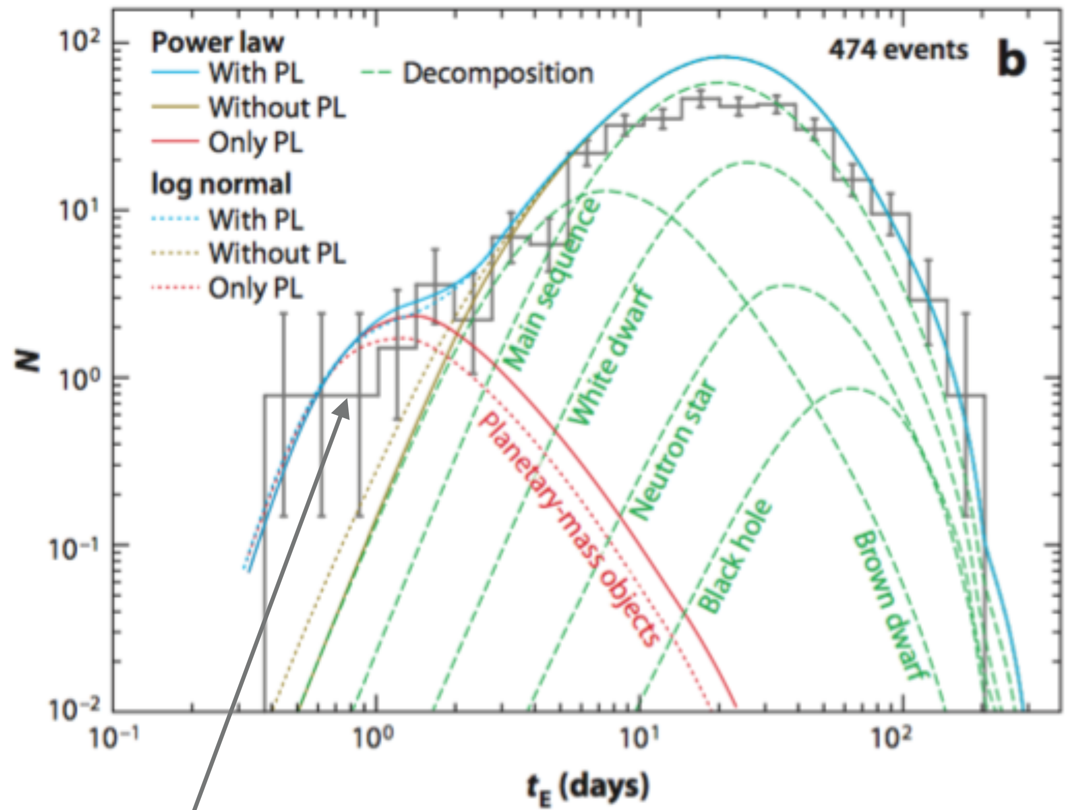

Theoretical estimate of the rate of microlensing events towards the galactic bulge

Distribution of microlensing event timescales observed by the MOA collaboration (2006-2007)

SOME IMPORTANT FACTS

- several collaborations have implemented the microlensing idea (proposed by B. Paczynski). These groups have monitored the galactic bulge and the Magellanic Clouds searching for microlensing events
- the relatively high rate of detections favored a barred model of the galaxy
- Towards the Magellanic Clouds, no ‘short’ events (timescales from a few hours up to 20 days) have been seen by any group. This places strong limits on ‘Jupiters’ in the dark halo: specifically, compact objects in the mass range 10^{-6}–0.05 solar masses contribute less than 10% of the dark matter around our Galaxy. This is a very important result, as these objects were previously thought to be the most plausible form of baryonic dark matter, and (for masses below 0.01 solar masses) they would have been virtually impossible to detect directly.

SOME IMPORTANT FACTS

- With the possible exception of MOA's free floating planets, generally, all the detected microlensing events are consistent with known stellar populations. Black holes can contribute up to 2% of the total mass of the halo.
- The recent detection of gravitational waves from merging BHs with intermediate masses has revived the idea of BHs as dark-matter candidates. For such lenses the time scale of the events would be large so that past microlensing surveys would not have been sensitive to them.

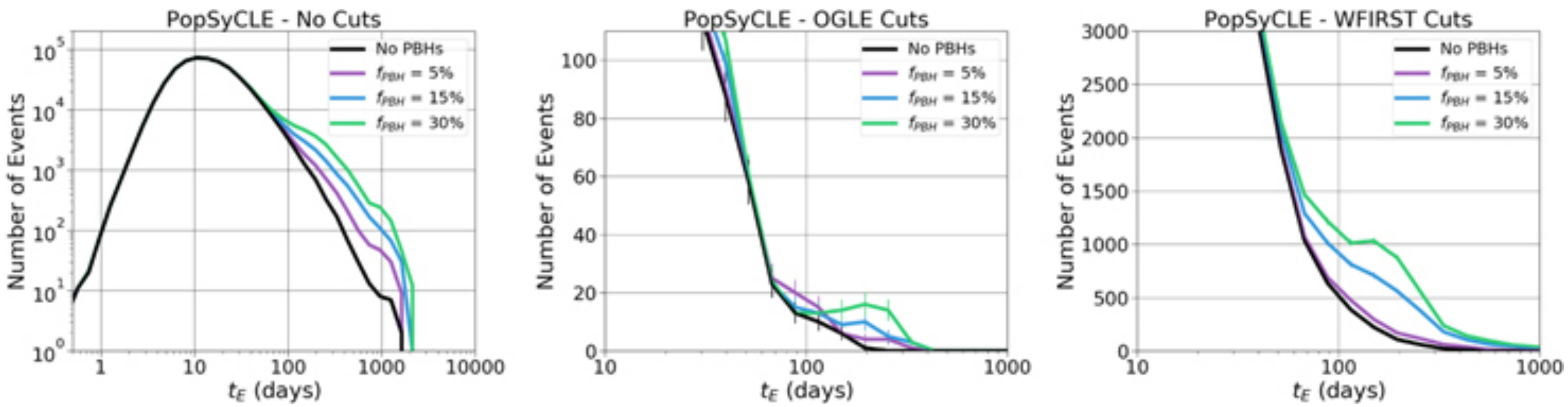

Lu et al. 2019